Supporting Information:
Exploring biotransformation of micropollutants in three freshwater phytoplankton species

Michael A. Stravs[†‡], Francesco Pomati[†§], Juliane Hollender[†‡*]

[†]Eawag Swiss Federal Institute of Aquatic Science and Technology, Überlandstrasse 133, 8600 Dübendorf, Switzerland

[‡]Institute of Biogeochemistry and Pollutant Dynamics, Universitätstrasse 16, ETH Zürich, 8092 Zürich, Switzerland

[§]Institute of Integrative Biology, ETH Zürich, Universitätstrasse 16, 8092 Zürich, Switzerland

* Corresponding Author

Überlandstrasse 133, 8600 Dübendorf, Switzerland

phone: +41 58 765 5493; fax: +41 58 765 5893; e-mail: juliane.hollender@eawag.ch

Summary: 36 pages, 9 tables, 6 figures

Table of Contents

List of Tables and Figures

S1. Supplementary Materials and Methods

Culture medium. Woods Hole Combo (WC) medium (as modified by Guillard and Lorenzen [1]) was prepared as follows: A solution of 1 mM $NaNO_3$, 250 µM $CaCl_2$, 150 µM $MgSO_4$, 150 µM $NaHCO_3$, 50 µM K_2HPO_4, 390 µM H_3BO_3, 11.7 µM Na_2EDTA, 11.7 µM $FeCl_3$, 10 nM $CuSO_4$, 76.5 nM $ZnSO_4$, 42 nM $CoCl_2$, 910 nM $MnCl_2$, 26 nM Na_2MoO_4, 98 nM Na_3VO_4, 0.5 mM TES (2-[[1,3-dihydroxy-2-(hydroxymethyl)propan-2-yl]amino]ethanesulfonic acid) in deionized water was prepared from 115 mg TES and 1000x stock solutions of the remaining constituents. The medium was sterilized by autoclaving (30 min at 121°C). Modified versions were prepared by replacing TES by 100 mL 0.1M MOPS (3-(N-morpholino)propanesulfonic acid) buffer stock solution, pH 7.5, per L of medium (Woods Hole Combo + MOPS, WC+M medium), or by replacing TES by 100 mL 0.1M pH 7.5 per L of medium, and 1 mM $NaNO_3$ by 1 mM NH_4Cl (Woods Hole Combo + Ammonia + MOPS, WC+A+M medium).

Experiments – small scale, *Mcy/Syn* mixtures. *Mcy* and *Syn* cultures were sampled at comparable optical densities and mixed 1:1. In 20 mL online vials, 3 mL of *Mcy/Syn* mixture were diluted with 3 mL fresh WC medium. For control samples, 6 mL of fresh WC or WC+M medium was added to 20 mL online vials. A chemical mixture or solvent control (see below) was added to a final concentration of 10 µg/L per compound and sample. To each sample, a stressor chemical or vector control was added (see below). The vials were capped with a non-fixed crimp cap and a tissue cover, and incubated as for single species experiments..

Immediately after addition of the chemical mixture (t0) and after timepoints up to a week (see below) samples were taken for chemical analysis and cell density measurement. For chemical analysis, 500 or 750 µL of well mixed culture were sampled into a HPLC vial and frozen until measurement. For cell density measurement, 200 uL per culture were sampled into a 96-well plate and optical density at 680 nm and 750 nm was measured (SpectraMax 190, Molecular Devices, Sunnyvale CA).

Experiments – small scale: sample preparation. The frozen samples were thawed and lysed in the ultrasonic bath for 5 min at 37°C. 150 uL of well-mixed sample were added to a 300 uL HPLC insert in an 1.5 mL Eppendorf vial and subsequently centrifuged 5' at 9000 rpm. 100 uL SN were diluted into 20 mL nanopure H_2O and fortified with internal standard (IS) mixture (total final absolute amount 1 ng IS per substance and sample).

pH controlled degradation experiment. Two culture vials were prepared with WC+M medium (pH 7.5), one sample was prepared with WC medium (pH 7.2). As a control, two culture vials with WC+M medium and one with WC medium were prepared and autoclaved. To all samples, chemical mixture 1 was added to a final concentration of 10 µg/L per compound. Samples were taken at 0, 2.5, 4, 24, 32, 50 and 74 hours.

Chemical stressor experiment – 3 stressors. 14 culture vials were prepared with WC medium. To 7 vials, chemical mixture 1 was added to a final concentration of 10 µg/L per compound; to the other 7 vials, chemical mixture 2 was added instead. To 6 of the 7 vials for each mixture, a chemical stressor (atrazine, irgarol or triclosan) was added to a final concentration of 10 ng/L (3 vials, one each, from 1 µg/L in EtOH) or 100 ng/L (3 vials, one each, from 10 µg/L in EtOH).To the last vial, no stressor (only equivalent EtOH) was added. As a control, one vial each was prepared without culture, with WC medium, and either chemical mixture 1 or 2 (medium control); and two vials were prepared with culture and WC medium and no chemical mixture (biological control). Samples were taken after 0, 1, 3, 5 and 7 days.

Chemical stressor experiment – atrazine only. 8 culture vials were prepared with WC medium. To 4 vials each, chemical mixture 1 or 2 was added to a final concentration of 10 µg/L per compound. To 2 vials each, atrazine (final concentration 100 ng/L, from 10 µg/L in EtOH)

was added; to the 2 other vials, no atrazine (only EtOH) was added. As a control, 4 vials were prepared without culture, with WC medium, 100 ng/L atrazine, and either chemical mixture 1 or 2 (two each, medium control); and 4 vials were prepared with culture and WC medium, no chemical mixture, and 100 ng/L atrazine (2 vials) or equivalent EtOH (2 vials) was added. Samples were taken after 0, 1, 3 and 5 days.

CBDZ: solvent exchange experiment. 8 culture vials were prepared with WC medium (5 mL volume, otherwise as above). To 2 vials each, Mix 1 (in EtOH), CBDZ alone in EtOH, CBDZ in isopropanol were added to a final concentration of 10 µg/L per compound (spike volume 50 µL); to two vials, EtOH alone (50 µL) was added (biological control). As a control, 3 vials were prepared with WC medium. To two, Mix 1 was added to a final concentration of 10 µg/L per compound; to one, CBDZ in EtOH was added to a final concentration of 10 µg/L. Samples were taken after 0, 1, 2 and 3 days.

Chemical analysis: Online SPE cartridge. An empty stainless steel SPE cartridge (20 mm x 2.1 mm, BGB) was filled with 9 mg Oasis HLB (15 µm particle diameter; Waters, USA) and a second layer of 9 mg of a 1:1:1.5 mixture of Strata X-AW (33 µm particle diameter), Strata X-CW (25 µm; both Phenomenex, Aschaffenburg, Germany), and Isolute ENV+ (70 µm; Biotage, Uppsala, Sweden).

Chemical analysis: source parameters. Source parameters were as follows: spray voltage: 4 kV (positive mode) or 3 kV (negative mode), capillary temperature: 320 °C, sheath gas: 40, auxiliary gas: 10, spare gas: 0, probe heater temperature: 50 °C, S-Lens RF level: 50. Calibration of the mass spectrometer was performed in positive and negative mode using an in-house amino acid / oligopeptide calibration solution.

Chemical analysis: Quantification and screening, method parameters For initial quantification measurements, data was acquired in polarity switching mode with data-dependent acquisition. Parameters were as follows: MS resolution: 70000, MS AGC target: 1×10^6, MS maximum injection time: 50 ms, mass range: m/z = 100-1500, loop count for MS2 acquisition: 3 (positive), 2 (negative), MS^2 resolution: 17500, MS^2 AGC target: 1×10^5, MS^2 maximum injection time: 50 ms, MS^2 isolation window: 1 Da, underfill ratio: 1%, MS^2 intensity threshold: 2×10^4, dynamic exclusion: 10 s, “pick others”: enabled.

Chemical Analysis: Spectra acquisition for compound identification, method parameters. Using inclusion lists, putative transformation products were fragmented in positive and negative mode at collision energies of 15, 30, 45, 60, 75, 90, 120, 150, 180 in time windows of 0.8 min around the expected retention time. Parameters were as follows: Full MS (positive and negative): MS resolution: 70000, MS AGC target: 5×10^5, MS maximum injection time: 50 ms, mass range: m/z = 70-1050. DIA (positive and negative): MS^2 resolution: 17500, MS^2 AGC target: 2×10^5, MS^2 maximum injection time: 50 ms, MS^2 isolation window: 1 Da, loop count: 9 × number of compounds measured.

Gene family search. Gene sequences associated to a gene family were retrieved from the JGI Integrated Microbial Genomes & Microbiome samples database (https://img.jgi.doe.gov/)[2,3]. In “Cassette Search”, genomes from domain “Bacteria”, selection “Cyanobacteria” (Finished, Permanent Draft and Draft) were chosen. Using the “Pfam” protein cluster option, genomes were searched for “pfam03321” (GH3 gene family), “pfam04055” (radical SAM gene family) or “pfam02310,pfam04055” (Logical Operator “And”; cobalamin binding domain and radical SAM superfamily, corresponding to radical SAM class B family.)

Estimation of environmental transformation rates. An estimated biomass-normalized first-order transformation rate equivalent was calculated from the final remaining fraction of compound (C/C_0), the experiment duration (t), and the average dry biomass during the experiment (B). From equation (1), the rate results as equation (2).

$$C = C_0\, e^{-k\, t\, B} \quad (1)$$

$$\mathrm{k} = \frac{-\log C/C_0}{B\, t} \quad (2)$$

For comparison with literature values from OECD 308/309 tests, DT_{50} values were converted to degradation rate constants using equation (3).

$$k = \frac{-\log 0.5}{DT_{50}} \quad (3)$$

Table S1 Used compounds , chemical formulas, molecular weights log Kow values, CAS numbers and sources.

Code	Name	Compound class	present in mixes		Formula	Molecular weight [Da]	Exact mass	log Kow		CAS	Vendor
			1	2							
ATE	Atenolol	Pharmaceutical	x	x	$C_{14}H_{22}N_2O_3$	266.3	266.163044	0.16	[2]	29122-68-7	Sigma-Aldrich
BEZ	Bezafibrate	Pharmaceutical	x	x	$C_{19}H_{20}ClNO_4$	361.8	361.108084	4.25	[4]	41859-67-0	Sigma-Aldrich
CBDZ	Carbendazim	Pharmaceutical	x	x	$C_9H_9N_3O_2$	191.2	191.069474	1.48	[1]	10605-21-7	Dr. Ehrenstorfer
MEF	Mefenamic acid	Pharmaceutical	x	x	$C_{15}H_{15}NO_2$	241.3	241.110284	5.12	[2]	61-68-7	Sigma-Aldrich
MPL	Metoprolol	Pharmaceutical	x	x	$C_{15}H_{25}NO_3$	267.4	267.183444	1.88	[2]	37350-58-6	Sigma-Aldrich
RAN	Ranitidine	Pharmaceutical	x	x	$C_{13}H_{22}N_4O_3S$	314.4	314.141262	0.27	[2]	66357-35-5	Sigma-Aldrich
TRA	Tramadol	Pharmaceutical	x	x	$C_{16}H_{25}NO_2$	263.4	263.188534	2.4	[2]	27203-92-5	Fluka
VFX	Venlafaxine	Pharmaceutical	x	x	$C_{17}H_{27}NO_2$	277.4	277.204184	3.28	[3]	93413-69-5	TRC Canada
VPL	Verapamil	Pharmaceutical	x	x	$C_{27}H_{38}N_2O_4$	454.6	454.283154	3.79	[2]	52-53-9	Sigma-Aldrich
AZY	Azoxystrobin	Strobilurin fungicide	x	x	$C_{22}H_{17}N_3O_5$	403.4	403.116824	2.5	[1]	131860-33-8	Fluka
FXS	Fluoxastrobin	Strobilurin fungicide	x	x	$C_{21}H_{16}ClFN_4O_5$	458.8	458.079326	2.86	[1]	361377-29-9	Dr. Ehrenstorfer
KME	Kresoxim-methyl	Strobilurin fungicide	x	x	$C_{18}H_{19}NO_4$	313.3	313.131404	3.4	[1]	143390-89-0	Dr. Ehrenstorfer
PYR	Pyraclostrobin	Strobilurin fungicide	x	x	$C_{19}H_{18}ClN_3O_4$	387.8	387.098584	3.99	[1]	175013-18-0	Fluka
TFL	Trifloxystrobin	Strobilurin fungicide	x	x	$C_{20}H_{19}F_3N_2O_4$	408.4	408.129694	4.5	[1]	141517-21-7	Dr. Ehrenstorfer
CYP	Cyproconazole	Azole fungicide (agric.)	x		$C_{15}H_{18}ClN_3O$	291.8	291.113844	3.09	[1]	94361-06-5	Dr. Ehrenstorfer
DIF	Difenoconazole	Azole fungicide (agric.)	x		$C_{19}H_{17}Cl_2N_3O_3$	406.3	405.064697	4.36	[1]	119446-68-3	Dr. Ehrenstorfer
EPO	Epoxiconazole	Azole fungicide (agric.)	x		$C_{17}H_{13}ClFN_3O$	329.8	329.073114	3.3	[1]	106325-08-0	Dr. Ehrenstorfer
FLU	Fluconazole	Azole fungicide (pharm.)	x		$C_{13}H_{12}F_2N_6O$	306.3	306.104064	0.4	[2]	86386-73-4	Dr. Ehrenstorfer
KET	Ketoconazole	Azole fungicide (pharm.)	x		$C_{26}H_{28}Cl_2N_4O_4$	531.4	530.148761	4.35	[2]	65277-42-1	Sigma-Aldrich
MET	Metconazole	Azole fungicide (agric.)	x		$C_{17}H_{22}ClN_3O$	319.8	319.14514	3.85	[1]	125116-23-6	Dr. Ehrenstorfer
PEN	Penconazole	Azole fungicide (agric.)	x		$C_{13}H_{15}Cl_2N_3$	284.2	283.064303	3.72	[1]	66246-88-6	Novartis
PRO	Propiconazole	Azole fungicide (agric.)	x		$C_{15}H_{17}Cl_2N_3O_2$	342.2	341.069784	3.72	[1]	60207-90-1	HPC Standards GmbH
TEB	Tebuconazole	Azole fungicide (agric.)	x		$C_{16}H_{22}ClN_3O$	307.8	307.145144	3.7	[1]	107534-96-3	Dr. Ehrenstorfer
SMZ	Sulfamethoxazole	Pharmaceutical:antibiotic	x		$C_{10}H_{11}N_3O_3S$	253.3	253.052114	0.89	[2]	723-46-6	Sigma-Aldrich

(agric.): in agricultural use, (pharm.) in pharmaceutical use
[1]: Data from Pesticide Properties Database[4]
[2]: Data from DrugBank[5]
[3]: Data from PubChem (CID: 5656)[6]
[4]: No experimental value for the log Kow of BEZ could be found; the used value is calculated using EPI-Suite[7]

Table S2 Parents and transformation products with internal standards used for quantification

Parent		Transformation product	CAS No.	Formula	m/z	RT [min]	internal standard
Atenolol	**ATE**			C14H22N2O3	267.1703	11.3	Atenolol-D7
	ATE	Atenolol-desisopropyl	81346-71-6	C11H16N2O3	225.1234	7.9	Carbamazepine-10-11-epoxide-13C-D2
	ATE, MPL	Atenolol/metoprolol acid	56392-14-4	C14H21NO4	268.1543	12.7	Atenolol/metoprolol acid-D5
Azoxystrobin	**AZY**			C22H17N3O5	404.1241	22.1	Azoxystrobin-D4
	AZY	Azoxystrobin acid	1185255-09-7	C21H15N3O5	390.1084	21.3	Azoxystrobin-D4, DEET-D10
Bezafibrate	**BEZ**			C19H20ClNO4	362.1154	22.6	Bezafibrate-D4
	BEZ	3-[(4-chlorobenzoyl)amino]-propanoic acid	108462-95-9	C10H10ClNO3	228.0422	19.5	Sulfadimethoxin-D4, Erythromycin-13C2
Carbendazim	**CBDZ**			C9H9N3O2	192.0768	13.9	Carbendazim-D4
Cyproconazole	**CYP**			C15H18ClN3O	292.1211	23.1	Epoxiconazole-D4
Difenoconazole	**DIF**			C19H17Cl2N3O3	406.0720	24.2	Propiconazole-D5
Epoxiconazole	**EPO**			C17H13ClFN3O	330.0804	23.4	Epoxiconazole-D4
Fluconazole	**FLU**			C13H12F2N6O	307.1113	17.5	Fluconazole-D4
Fluoxastrobin	**FXS**			C21H16ClFN4O5	459.0866	23.0	Epoxiconazole-D4
Ketoconazole	**KET**			C26H28Cl2N4O4	531.1560	19.2	Atomoxetin-D3, Erythromycin-13C2
Kresoxim-methyl	**KME**			C18H19NO4	314.1387	23.7	Epoxiconazole-D4
	KME	Kresoxim-methyl acid	181373-11-5	C17H17NO4	300.1230	23.4	Epoxiconazole-D4
Mefenamic acid	**MEF**			C15H15NO2	242.1176	24.7	Mefenamic acid-D3
Metconazole	**MET**			C17H22ClN3O	320.1524	24.2	Propiconazole-D5
Metoprolol	**MPL**			C15H25NO3	268.1907	15.6	Metoprolol-D7
Penconazole	**PEN**			C13H15Cl2N3	284.0716	23.9	Tebuconazole-D6
Propiconazole	**PRO**			C15H17Cl2N3O2	342.0771	24.0	Propiconazole-D5
Pyraclostrobin	**PYR**			C19H18ClN3O4	388.1059	24.0	Tebuconazole-D6
Ranitidine	**RAN**			C13H22N4O3S	315.1485	11.3	Ranitidine-D6
	RAN	Ranitidine S-oxide	73851-70-4	C13H22N4O4S	331.1435	7.0	Carbendazim-D4
	RAN	Ranitidine N-oxide	73857-20-2	C13H22N4O4S	331.1435	11.7	Carbendazim-D4
Sulfamethoxazole	**SMZ**			C10H11N3O3S1	254.0594	16.3	Sulfamethoxazole-D4
	SMZ	N-Acetyl-Sulfamethoxazole	21312-10-7	C12H13N3O4S	296.0700	17.9	N-Acetyl-Sulfamethoxazole-D5
Tebuconazole	**TEB**			C16H22ClN3O	308.1524	23.9	Tebuconazole-D6
Trifloxystrobin	**TFL**			C20H19F3N2O4	409.1370	24.2	Propiconazole-D5
	TFL	Trifloxystrobin acid	252913-85-2	C19H17F3N2O4	395.1213	23.9	Tebuconazole-D6 (*)

Tramadol	**TRA**			C16H25NO2	264.1958	15.5	Tramadol-D6
	TRA	N,N-didesmethyltramadol	931115-27-4	C14H21NO2	236.1645	16.1	Tramadol-D6
	TRA	N-desmethyltramadol	73806-55-0	C15H23NO2	250.1802	16.0	Tramadol-D6
	TRA	Tramadol N-oxide	147441-56-3	C16H25NO3	280.1907	16.0	Atrazine-desethyl-15N3
Venlafaxine	**VFX**			C17H27NO2	278.2115	17.2	Venlafaxine-D6
	VFX	N-desmethylvenlafaxine	149289-30-5	C16H25NO2	264.1958	17.3	Venlafaxine-D6
	VFX	N,N-didesmethylvenlafaxine	93413-77-5	C15H23NO2	250.1802	17.3	N,O-didesmethylvenlafaxine-D3
	VFX	N,O-didesmethylvenlafaxine	135308-74-6	C15H23NO2	250.1802	15.3	N,O-didesmethylvenlafaxine-D3
	VFX	O-desmethylvenlafaxine	93413-62-8	C16H25NO2	264.1958	15.2	O-desmethylvenlafaxine-D6
	VFX	Venlafaxine N-oxide	1094598-37-4	C17H27NO3	294.2064	17.8	Venlafaxine-D6
Verapamil	**VPL**			C27H38N2O4	455.2904	18.2	Verapamil-D6
	VPL	D617	34245-14-2	C17H26N2O2	291.2067	23.2	Verapamil-D6, Atorvastatin-D5

(*): quantified by relative peak area in single species experiments

Table S3 Suspect screening lists used for transformation product prediction.

Type	Name	Mass difference	Loss	Gain	Formula difference	Description
	parent	0.0000				no change
Reductions, oxidations, skeleton substitutions (CHNO)						
	oh	15.9949		O	O1	Hydroxlation
	deme	-14.0157	CH3	H	C-1H-2	Demethylation
	deet	-28.0313	C2H5	H	C-2H-4	Deethylation
	deh2	-2.0157	H2		H-2	General reduction
	h2	2.0157		H2	H2	General oxidation
	deh2o	-18.0106	H2O		H-2O-1	Dehydration
	h2o	18.0106		H2O	H2O1	Hydration
	deco2	-43.9898	CO2		C-1O-2	Decarboxylation
	deno2	-44.9851	NO2	H	H1N-1O-2	Nitro group loss
	meoxi	29.9742	H	O2H	O2	Methyl oxidation to carboxylic acid
	deamin	-15.0109	H	NH2	N1H1	Deamination
	oxicooh	13.9793	H2	O	O1H-2	Alcohol oxidation to acid
	nitrored	-29.9742	O2	H2	H2O-2	Nitro reduction
	disnhox	0.9840	NH2	OH	O1N-1H-1	Amine to hydroxy (ipso-)substitution
	deipr	-42.0470	C3H7	H	C-3H-6	Isopropyl loss
	amin	-0.9840	OH	NH2	N1O-1H1	Hydroxy to amine (ipso-)substitution
Reductions, oxidations (Cl, F)						
	clXh	-33.9610	Cl	H	H1Cl-1	Reductive dechlorination
	disf	-17.9906	F	H	H1F-1	Reductive defluorination
	disclox	-17.9661	Cl	OH	O1H1Cl-1	Oxidative dechlorination
	disfox	-1.9957	F	OH	O1H1F-1	Oxidative defluorination
Conjugation-type reactions: methylation						
	me	14.0157	H	CH3	C1H2	Methylation
	et	28.0313	H	C2H5	C2H4	Ethylation / di-methylation
Conjugation-type reactions: amino acid conjugation						
	leu	113.0841	H2O	C6N1H13O2	C6N1H11O1	Leucine / isoleucine
	lys	128.0950	H2O	C6N2H14O2	C6N2H12O1	Lysine
	met	131.0405	H2O	C5N1S1H11O2	C5N1S1H9O1	Methionine
	phe	147.0684	H2O	C9N1H11O2	C9N1H9O1	Phenylalanine
	thr	101.0477	H2O	C4N1H9O3	C4N1H7O2	Threonine
	try	186.0793	H2O	C11N2H12O2	C11N2H10O1	Tryptophan
	val	99.0684	H2O	C5N1H11O2	C5N1H9O1	Valine
	arg	156.1011	H2O	C6N4H14O2	C6N4H12O1	Arginine
	his	137.0589	H2O	C6N3H9O2	C6N3H7O1	Histidine
	ala	71.0371	H2O	C3N1H7O2	C3N1H5O1	Alanine
	asn	114.0429	H2O	C4N2H8O3	C4N2H6O2	Asparagine
	asp	115.0269	H2O	C4N1H7O4	C4N1H5O3	Aspartate
	cys	103.0092	H2O	C3N1S1H7O2	C3N1S1H5O1	Cysteine
	glu	129.0426	H2O	C5N1H9O4	C5N1H7O3	Glutamate
	gln	128.0586	H2O	C5N2H10O3	C5N2H8O2	Glutamine
	gly	57.0215	H2O	C2N1H5O2	C2N1H3O1	Glycine
	pro	97.0528	H2O	C5N1H9O2	C5N1H7O1	Proline
	ser	87.0320	H2O	C3N1H7O3	C3N1H5O2	Serine
	tyr	163.0633	H2O	C9N1H11O3	C9N1H9O2	Tyrosine
	adda	313.2042	H2O	C20H29NO3	C20N1H27O2	ADDA [1]
Conjugation-type reactions: other						
	gluc	176.0321	H	C6H9O6	C6O6H8	Glucuronidation
	nac	42.0106	H	C2H3O	C2O1H2	(N-)acetylation
	sulf	79.9568	H	HSO3	S1O3	Sulfate conjugation
	gsh	305.0682	H	C10H15N3O6S	C10H15N3O6S1	Glutathione conjugation
	naccys	162.0225	H	C5H8NO3S	C5H8N1O3S1	(N-)acetylcysteine conjugation

[1] ADDA is a non-proteinogenic amino acid found in toxic cyanobacterial peptides, e.g. microcystin.[8]

S2. Supplementary Results

S2.1 Bioconcentration

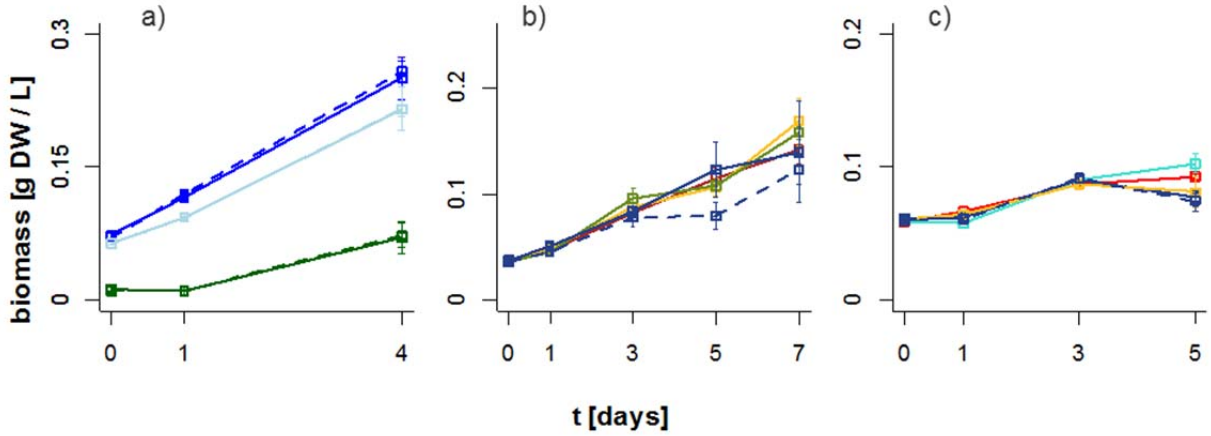

Figure S1 Growth curves for single culture experiments (a) and mixture experiments (b,c). a) Dark blue: Mcy, light blue: Syn, green: Chl. Solid lines: cultures treated with chemicals, dashed lines: chemical-free control. Note: The lines for Syn overlap completely, which is why the chemical control is not visible. b) Mixture experiments with stressors at 100 ng/L, blue: no stressor, yellow: atrazine, brown: irgarol, olive: triclosan, blue dashed: chemical-free control. c) Mixture experiments with stressors. Blue: no stressor; yellow: atrazine 100 ng/L; red: azoles 10 µg/L, turquoise: atrazine and azoles; blue dashed: chemical-free control.

Table S4: Mass balance of studied compounds after 4 days.

	Microcystis			Synechococcus			Chlamydomonas		
	medium	cells	TPs	medium	cells	TPs	medium	cells	TPs
Atenolol	95%	0%		87%	0%	ATE/MPL-A: 7%	102%	0%	
Azoystrobin	102%	0%		95%	0%		107%	0%	
Bezafibrate	96%	0%	BEZ-da: <1%*	93%			100%		BEZ-da: <1%*
Carbendazim (see S2.3)	99%			94%		(CBDZ-M: 1%*)	104%		
Cyproconazole	101%	0%		95%	0%		102%	0%	
Difenoconazole	83%	0%		77%	4%		98%	2%	
Epoxyconazole	97%	0%		92%	1%		100%	0%	
Fluconazole	97%			94%			101%		
Fluoxastrobin	103%	0%		90%	2%		108%	0%	
Ketoconazole (see S2.4)	23%	3%	(7%*)	48%	0%	(7%*)	75%	1%	(8%*)
Kresoxim-methyl	1%	0%	KME-A: 101%	68%	1%	KME-A: 29%	94%	0%	KME-A: 14%
Mefenamic acid	89%	0%		85%		MEF-Glu: 9%*	96%		
Metconazole	95%	0%		93%	0%		104%	0%	
Metoprolol	94%	0%		93%			86%		ATE/MPL-A: 4% (medium) 2% (cells) MPL-dm: 6%*
Penconazole	96%	0%		94%	0%		102%	0%	
Propiconazole	96%	0%		95%	0%		102%	0%	
Pyraclostrobin	85%	2%		61%	12%		96%	1%	
Ranitidine	84%	0%	RAN-dm: 4%*	89%	0%		94%	0%	
Sulfamethoxazole	66%	0%	SMZ-DHPt: 2%* SMZ-Pt: 3%* SMZ-PtO: 3%*	38%	0%	SMZ-AcOH: 2%*	98%	0%	
Tebuconazole	96%			93%			102%		
Tramadol	119%			117%			125%		
Trifloystrobin	2%	0%	TFL-A: 101%*	49%	8%	TFL-A: 28%*	96%	1%	TFL-A: 7%*
Venlafaxine	101%			100%			106%		
Verapamil	69%	0%	VPL-da: 1%	90%	0%	VPL-da: <1%	97%	0%	VPL-da: <1%

“medium”: parent substance in medium. “cells”: parent substance in cells. “TPs”: transformation products. (*): quantified using peak area ratio. Unless otherwise noted, TPs were only found in medium. Values are the mean of three replicates.

Table S5 Individual apparent log bioconcentration factors for each compound in the three species Mcy, Syn and Chl.

	Mcy	Syn	Chl
ATE	2.2	1.4	1.5
AZY	0.9	1.5	2.3
BEZ	1.1	-	-
CBDZ	-	-	-
CYP	1.3	1.7	1.9
DIF	2.5	2.8	3.3
EPO	1.4	1.7	2.5
FLU	-	-	-
FXS	1.7	2.4	2.3
KET	2.7	2.5	3.1
KME	-	-	2.7
MCZ	1.6	2.0	2.4
MEF	2.2	-	-
MPL	1.4	-	-
PEN	1.5	-	2.2
PRO	1.0	-	-
PYR	3.2	3.1	2.9
RAN	1.3	-	1.9
SMZ	1.5	1.9	-
TEB	-	-	-
TFL	-	3.0	2.9
TRA	-	-	-
VFX	-	-	-
VPL	2.1	1.9	1.8

Mean log BCF were calculated from the point of apparent equilibration.
No log BCF was calculated for

- CBDZ, FLU, TRA, VFX (all species), BEZ, MPL, TEB, MEF (some species) because internal concentrations in cells were negligible
- KME for Mcy and Chl, and TFL for Mcy, because degradation was too rapid to reliably determine an (apparent) BCF

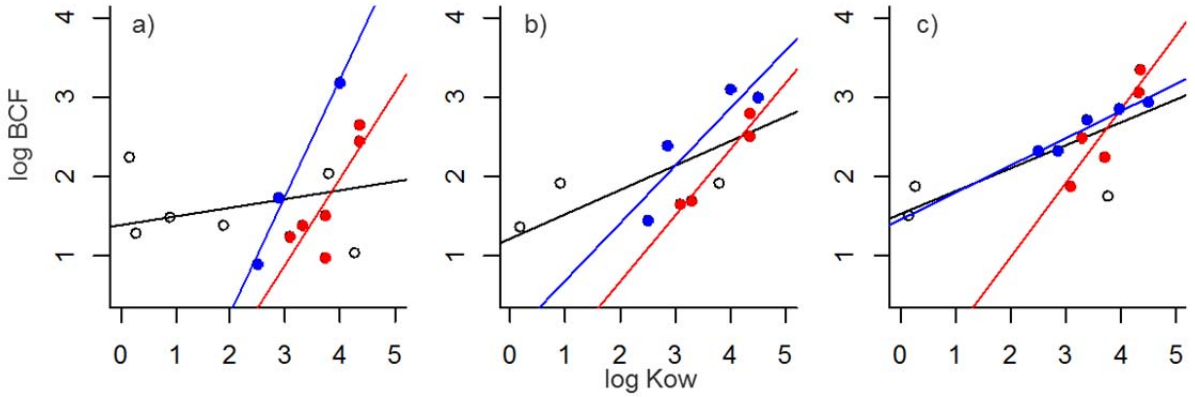

Figure S2 Log bioconcentration factor in dependence of log K_{ow} for a) Mcy, b) Syn and c) Chl. Red filled circles: azole fungicides; blue filled circles: strobilurin fungicides, black open circles: remaining compounds. Red, blue and black line: linear correlation for azole fungicides only (red), strobilurin fungicides only (blue), or all compounds (including azole and strobilurin fungicides; black).

Table S6 log K_{ow} correlations to apparent bioconcentration factor.

		log BCF = a + b * log K_{ow}			adjusted		
Species	**Chem**	**a**	**b**	**R^2**	**R^2**	**p (b ≠ 0)**	
Mcy	all	1.39	0.11	0.06	-0.01	0.39	
Syn	all	1.23	0.30	0.49	0.43	0.017	(*)
Chl	all	1.53	0.29	0.53	0.49	0.004	(**)
Mcy	azoles	-2.38	1.09	0.71	0.63	0.036	(*)
Syn	azoles	-0.97	0.83	0.95	0.93	0.024	(*)
Chl	azoles	-0.86	0.92	0.82	0.76	0.035	(*)
Mcy	strobilurins	-2.64	1.47	0.98	0.97	0.083	
Syn	strobilurins	-0.01	0.72	0.80	0.71	0.1	
Chl	strobilurins	1.47	0.34	0.92	0.90	0.009	(**)

p (b ≠ 0): p value for slope of the linear regression log BCD = a + b * log K_{ow}. (*): $p < 0.05$; (**): $p < 0.01$

S2.2 Transformation product identification

Table S7 Analytical summary of found transformation products.

Parent		m/z		Identification		MS2 spectra (MassBank)
TP	**Formula**	**$[M+H]^+$**	**$[M-H]^-$**	**level**	**RT**	**(Bold: annotated spectrum in SI)**
KME	*C18H19NO4*	314.1386	(312.1240)			
KME-A	C17H17NO4	300.1234	(298.1088)	1	23.6	
TFL	*C20H19F3N2O4*	409.1368	(407.1222)			
TFL-A	C19H17F3N2O4	395.1213	(393.1067)	1	24.1	
CBDZ	*C9H9N3O2*	192.0767				
CBDZ-M	C10H11N3O2	206.0926		2b	15.6	ET270101..09 (pos) **ET270102**
MEF	*C15H15NO2*	242.1175	240.1029			
MEF-Glu	C20H22N2O5	371.161	369.1464	3	23.3	ET320101..09 (pos) ET320151..59 (neg) **ET320152**
SMZ	*C10H11N3O3S*	254.0593	252.0447			
SMZ-DHPt	C17H18N8O4S	431.1244	429.1098	3	16.6	
SMZ-Pt	C17H16N8O4S	429.1090	427.0944	2b	16.7	ET310201..09 (pos) ET310251..59 (neg) **ET310201..09 (merged)**
SMZ-PtO	C17H14N7O5S	430.0930	428.0784	3	16.8	ET310301..09 (pos) ET310351..59 (neg) **ET310201..09 (merged)**
SMZ-Ac	C12H13N3O4S	296.0700	294.0554	1		
SMZ-AcOH	C12H13N3O5S	312.0649	310.0503	3	16.8	ET310401..09 (pos) ET310451..59 (neg) **ET301402**
MPL	*C15H25NO3*	268.1906			15.5	
ATE	*C14H22N2O3*	267.1702			11.4	
MPL/ATE-A	C14H21NO4	268.1542		1	13.6	
MPL-dm	C14H23NO3	254.1750		2b	13.1	ET280101..09 (pos)
BEZ	*C19H20ClNO4*	362.1152	360.1006		22.7	
BEZ-da	C15H14ClNO2	276.0787	(274.0641)	2b	21.4	ET290101..09 (pos) **ET290103**
BEZ-M	C20H22ClNO4	376.1310		2b	23.3	ET290201..09 (pos) **ET290202**

Note: All retention times are given as found in the initial measurement. Retention times in the MassBank spectra may slightly differ if measured on a different chromatographic system, depending on system availability at the time. m/z values in parentheses: weak signal

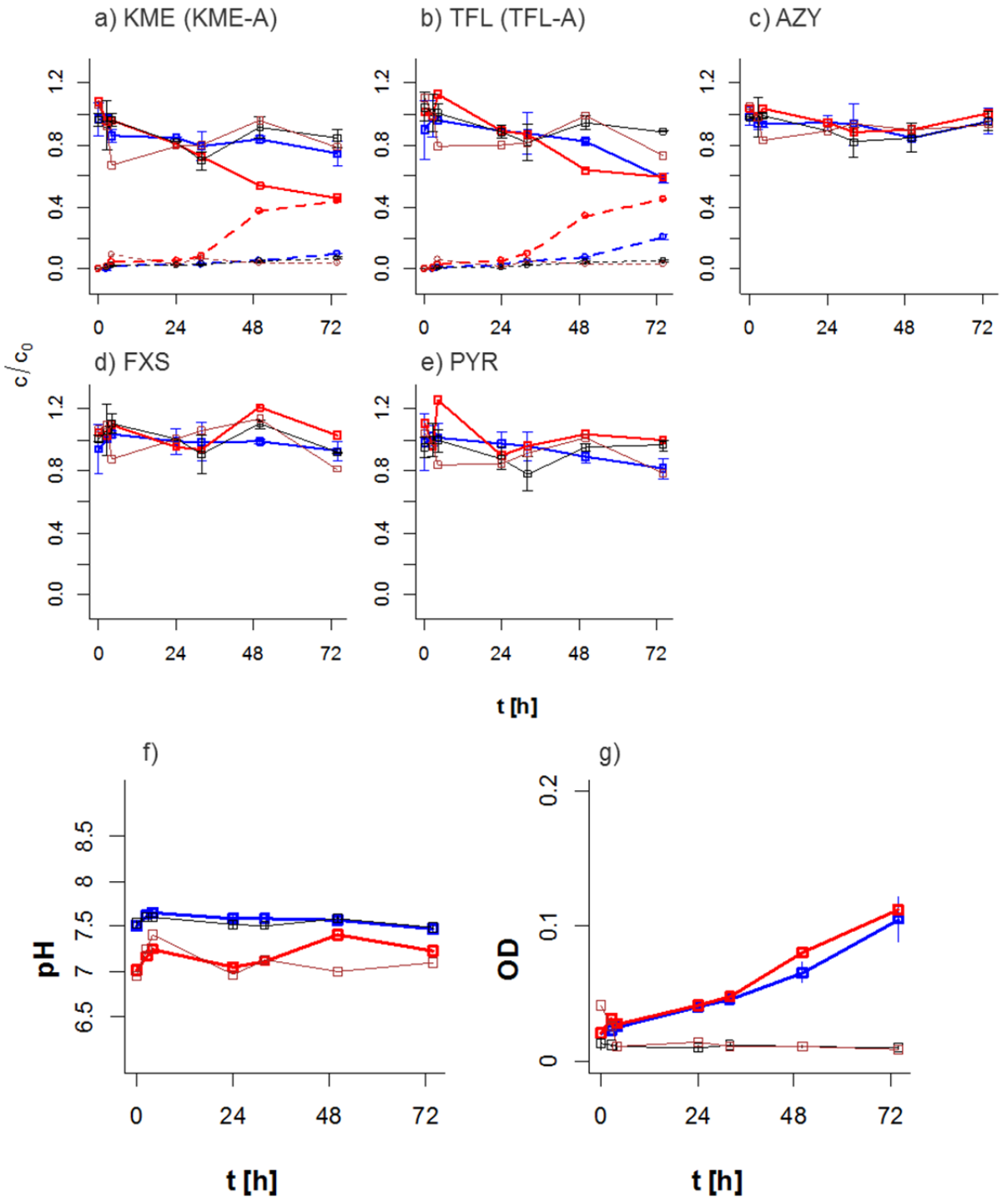

Figure S3 pH-controlled experiments for strobilurin fungicides. Top 5 plots, a)-e): KME, TFL, AZY, FXS, PYR; dashed: KME-A, TFL-A. f) pH over time g) biomass (determined from optical density at 750 nm) over time. Blue: nominal pH 7.5, red: nominal pH 7.2, black (narrow): autoclave control pH 7.5, brown (narrow): autoclave control pH 7.2.

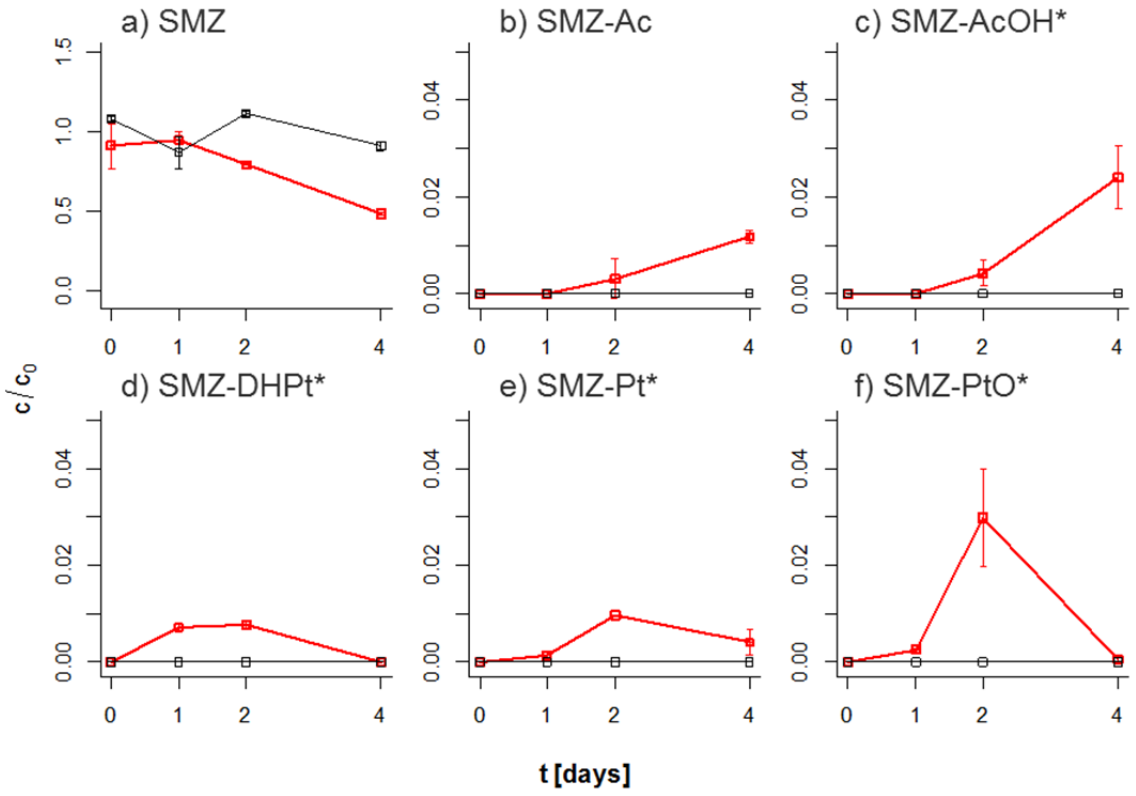

Figure S4 Sulfamethoxazole and metabolites in mixture experiments. a) SMZ, b) SMZ-Ac, c) SMZ-AcOH, d) SMZ-DHPT, e) SMZ-Pt, f) SMZ-PtO. Red: Mcy+Syn mixture, black: medium control. c/c_0 values are concentrations, or transformation product amounts semiquantified via peak area (marked *), relative to average initial parent concentration.

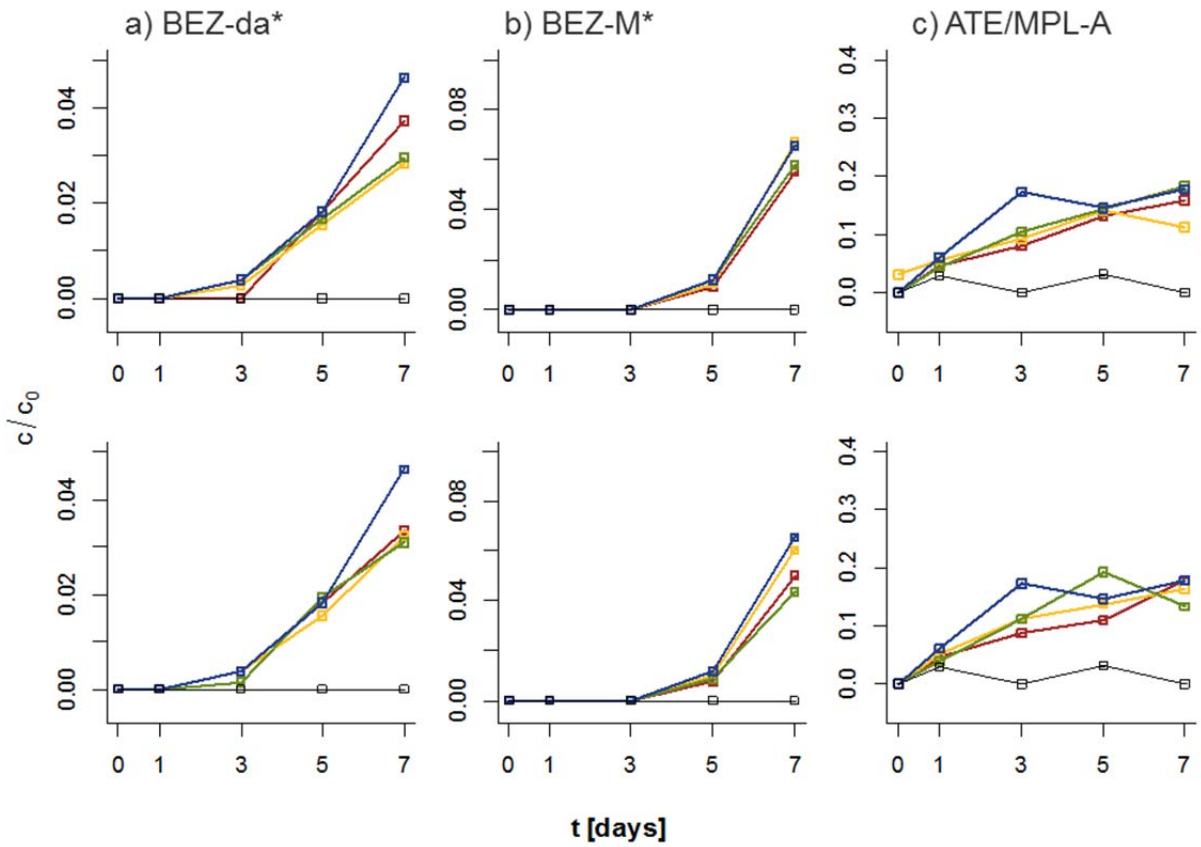

Figure S5 Formation of BEZ-da (a), BEZ-M (b) and ATE/MPL-A (c) under chemical stress. Blue: no stressor, yellow: atrazine, brown: irgarol, olive: triclosan, black: medium control. Top: 100 ng/L stressor concentration, bottom: 10 ng/L stressor concentration. All experiments without azole mixture. c/c_0 values are concentrations, or transformation product amounts semiquantified via peak area (marked *), relative to average initial parent concentration.

S2.3 Enzymatic transesterification of CBDZ with ethanol

In single species experiments with *Syn* and in *Mcy*+*Syn* combined experiments, a product (CBDZ-M, $[M+H]^+$ 206.0926, RT: 15.6 min) consistent with a methylation product of CBDZ was found by suspect screening (Figure S6). Methylation of a nitrogen by a methyltransferase would be the most obvious explanation for the product. However, both the most straightforward manual interpretation of the spectrum and in-silico MS^2 spectra (using CFM-ID[9,10], see SI S3.2, SI S3.3) of possible structures suggest methylation on the methyl ester carbon, whereas no fragments provide evidence for a methyl group on the N.

This was initially hypothesized to be a carbon methylation reaction, which can be performed by radical S-adenosylmethionine-dependent enzymes (RS enzymes)[11]. However, further experiments showed that formation of CBDZ-M is abolished when CBDZ is dissolved in isopropanol instead of ethanol, whereas small amounts of a corresponding product with addition of C_2H_4 was found. Therefore, the CBDZ-M product is likely formed by a transesterification with ethanol, rather than by methylation of the terminal CH3. Neither of these products is formed abiotically, supporting an enzymatic reaction (Figure S6).

This reaction shows an interesting xenobiotic pathway in Synechococcus. Enzymatic transesterification by ethanol is known, for example, for cocaine in humans and mice[12] Although this reaction is not relevant under environmental conditions reactions with other biological alcohols could potentially be of interest. Other TPs for CBDZ were not found; in particular there was no evidence for the formation of the hydrolysis product 2-aminobenzimidazole, which is commonly found in microbial biotransformation[13].

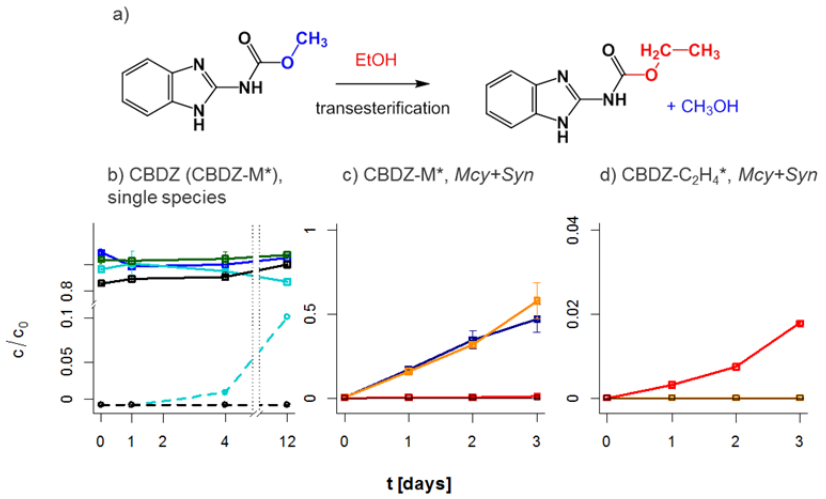

Figure S6 Transesterification of CBDZ with EtOH. a) suggested reaction. b) CBDZ biotransformation in single-species experiments. Solid lines: CBDZ, dashed lines: CBDZ-M. Blue: *Mcy*, turquoise: *Syn*, green: *Chl*. Black: medium control. c)-d) CBDZ TP formation in solvent exchange experiments. c) CBDZ-M, d) CBDZ-C_2H_4. Dark blue: *Mcy*+*Syn*, Mix 1 in EtOH. Orange: *Mcy*+*Syn*, CBDZ in EtOH. Red: *Mcy*+*Syn*, CBDZ in isopropanol. Black: abiotic control. c/c0 values are parent concentration, or transformation product semiquantified via peak area (marked *), relative to average initial concentration.

S2.4 Abiotic transformation of KET

For KET, 25-75% dissipation after 4 days and >75% dissipation after 12 days was observed in single species experiments and a single TP ($[M+H]^+$ 533.1353) was found. However, the substance was not consistently stable in medium controls, and the TP was found also in controls where KET loss was observed. While KET is documented to be long-term stable in aqueous solutions from pH 5-9 under presence of minimal amounts of antioxidant[14], no information is available on its stability in solutions similar to WC medium; abiotic oxidation, potentially by indirect photochemistry, is a likely source for the TP.

S2.5 Estimation of environmental transformation rates

Estimated environmental biomass-normalized transformation rates (Table S8) were calculated for ATE as described in Supplementary Materials and Methods. To compare calculated rates with known values, DT_{50} values from literature were converted to degradation rates as described (Table S9). Phytoplankton biomass values for the eutrophic lake Greifensee (Switzerland) in the range of 4 mm^3/L were used as a reference[15]. Using 0.47 $pg/\mu m^3$ as a wet biovolume to dry weight conversion estimate[16], a dry weight equivalent of 2 mg/L can be obtained. The contribution of phytoplankton was then estimated by multiplying the biomass-normalized rate with the biomass, and diving the obtained rate by the rate derived from DT_{50} values.

It should be noted that the observed data qualitatively do not match neither a first-order decay nor a pure biomass-dependent degradation, but likely involve some regulation dynamics. Therefore these values are to be seen as the roughest of estimates, however they should serve to get an order-of-magnitude estimate of the relevance of the observed reactions to environmental situations.

Table S8 Estimation of environmental transformation rates for ATE

	% remaining	**log degradation**	**time** [days]	**biomass** [g/L]	**norm. rate** [$(d \times g/L)^{-1}$]
ATE (Syn)	65	-0.19	12	0.2	0.08
ATE (Mcy+Syn)	85	-0.07	5	0.1	0.14

"norm. rate": estimated dry biomass normalized first order degradation rate.

Table S9 Estimation of phytoplankton contribution to environmental transformation rates.

	norm. rate [$(d \times g/L)^{-1}$]	**biomass** [g/L]	**env.rate** [d^{-1}]	**DT_{50}** [d]	**lit. rate** [d^{-1}]	**contribution** [%]
ATE (Syn)	0.08	0.002	1.6×10^{-4}	12.8-69.3[17]	0.004 to 0.025	0.6 to 4
ATE (Mcy+Syn)	0.14		2.8×10^{-4}			1 to 7

"norm. rate": estimated dry biomass normalized first order degradation rate. "env.rate": estimated contribution to environmental first-order degradation with given biomass. "lit. rate": Literature DT_{50} converted to first-order degradation rate.

S3. Spectra and Data for Transformation Products

S3.1 Structure Elucidation of MEF-Glu

MS2 spectrum, negative mode, parent [M-H]- 369.1465, collision energy NCE 30. Automated formula annotation (RMassBank) MassBank reference: ET320152.

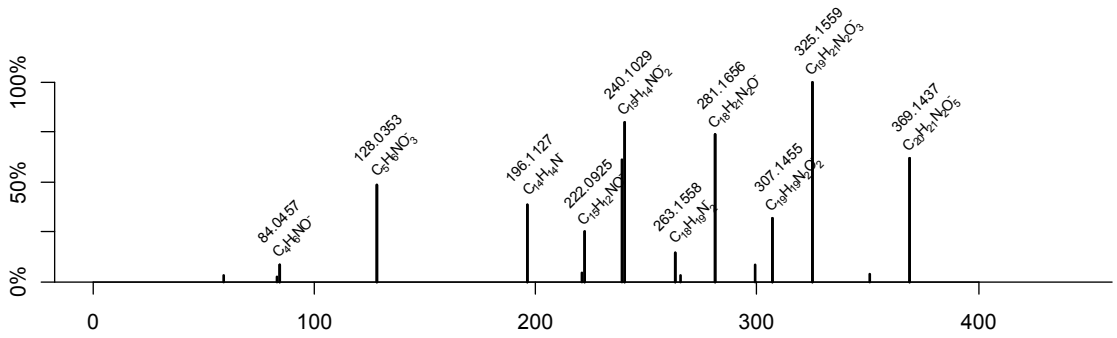

Proposed Structure (modification in red) **and Fragmentation:**

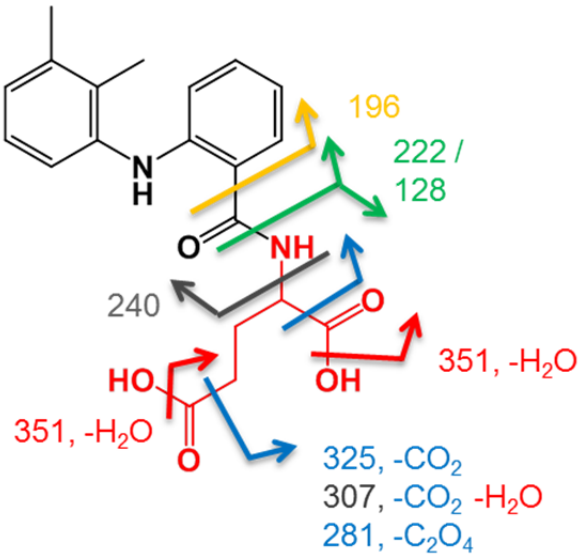

Confidence level: Level 3

Additional evidence for structure interpretation:

In positive mode, dominant fragment 224 (loss of amino acid moiety).

S3.2 Structure Elucidation of CBDZ-M

MS2 spectrum, positive mode, parent $[M+H]^+$ 206.0924, collision energy NCE 30. Automated formula annotation (RMassBank). MassBank reference: ET270102

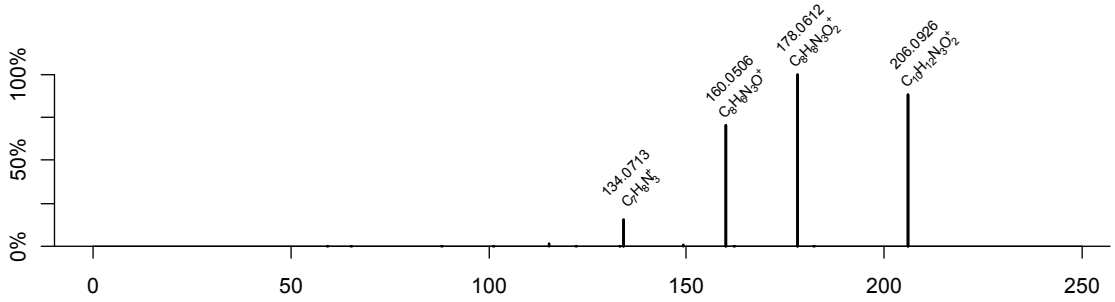

Proposed Structure (modification in red) **and Fragmentation:**

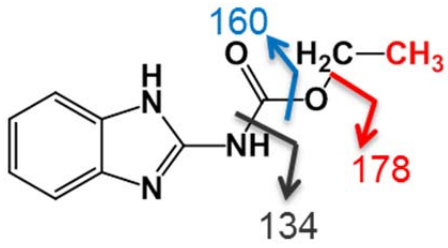

Confidence Level: Level 2b

Additional evidence for structure interpretation:

See SI S3.3, comparison with in-silico spectra by CFM-ID

As noted in the main text, this product could in theory be formed by “ethanolysis” of the methyl ester as a possible side reaction to hydrolysis. However, a corresponding hydrolysis product is not observed. For KME and TFL, which show marked hydrolysis, trace quantities of transformation products possibly formed by ethanolysis could be observed ($[M+H]^+$ 328.1543, RT: 24.2 min for the KME product KME-M, 423.1527, RT: 24.6 min for the TFL product TFL-M).

S3.3 Comparison of CBDZ-M spectrum to predicted CFM-ID spectra.

Top: MS2 spectrum, positive mode, parent $[M+H]^+$ 206.0924, merged spectra (collision energies NCE 15, 30, 45, 60, 75, 90) by absolute intensity. MassBank reference: ET270101-ET270109.

Bottom: In-silico MS2 spectrum, CFM-ID, positive mode, merged spectra (collision energy 10 eV, 20 eV, 40 eV).

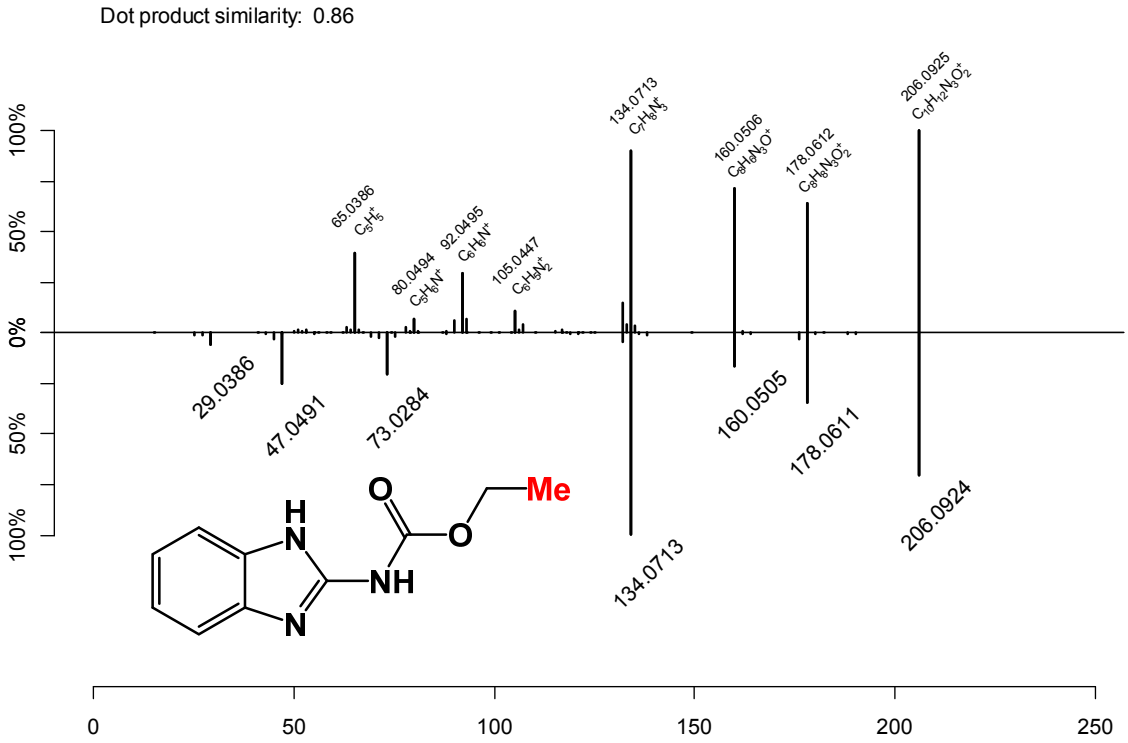

Top: MS2 spectrum, positive mode, parent $[M+H]^+$ 206.0924, merged spectra (collision energies NCE 15, 30, 45, 60, 75, 90) by absolute intensity. MassBank reference: ET270101-ET270109.

Bottom: In-silico MS2 spectrum, CFM-ID, positive mode, merged spectra (collision energy 10 eV, 20 eV, 40 eV).

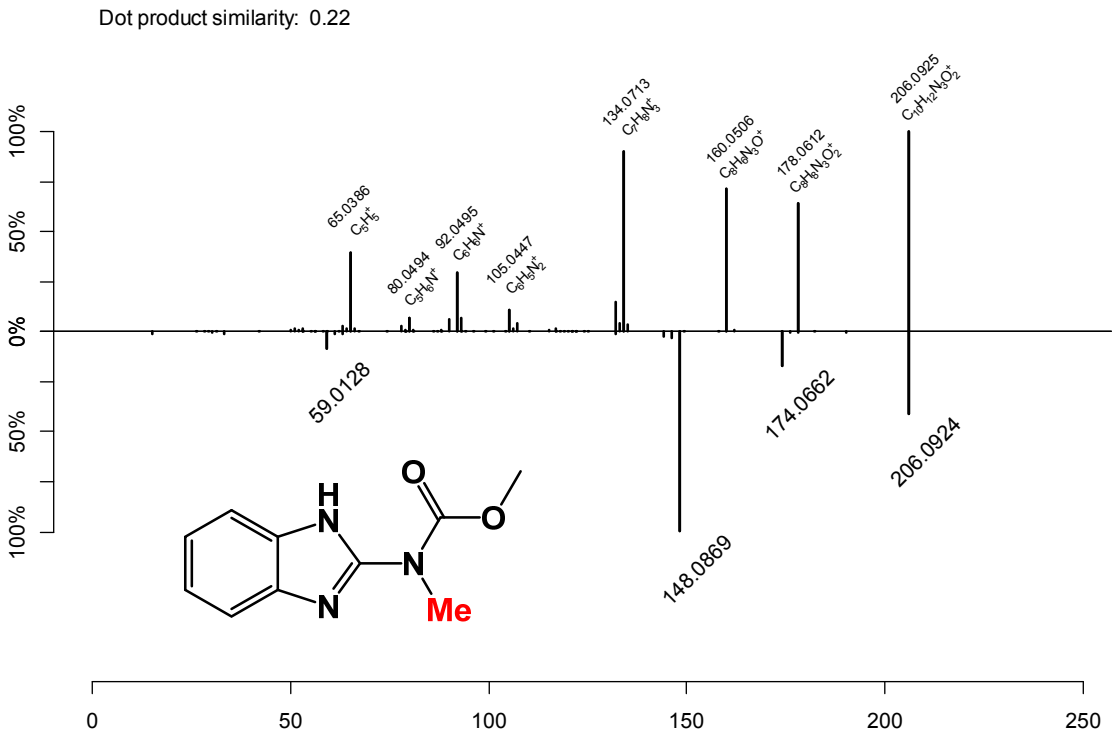

Top: MS2 spectrum, positive mode, parent $[M+H]^+$ 206.0924, merged spectra (collision energies NCE 15, 30, 45, 60, 75, 90) by absolute intensity. MassBank reference: ET270101-ET270109.

Bottom: In-silico MS2 spectrum, CFM-ID, positive mode, merged spectra (collision energy 10 eV, 20 eV, 40 eV).

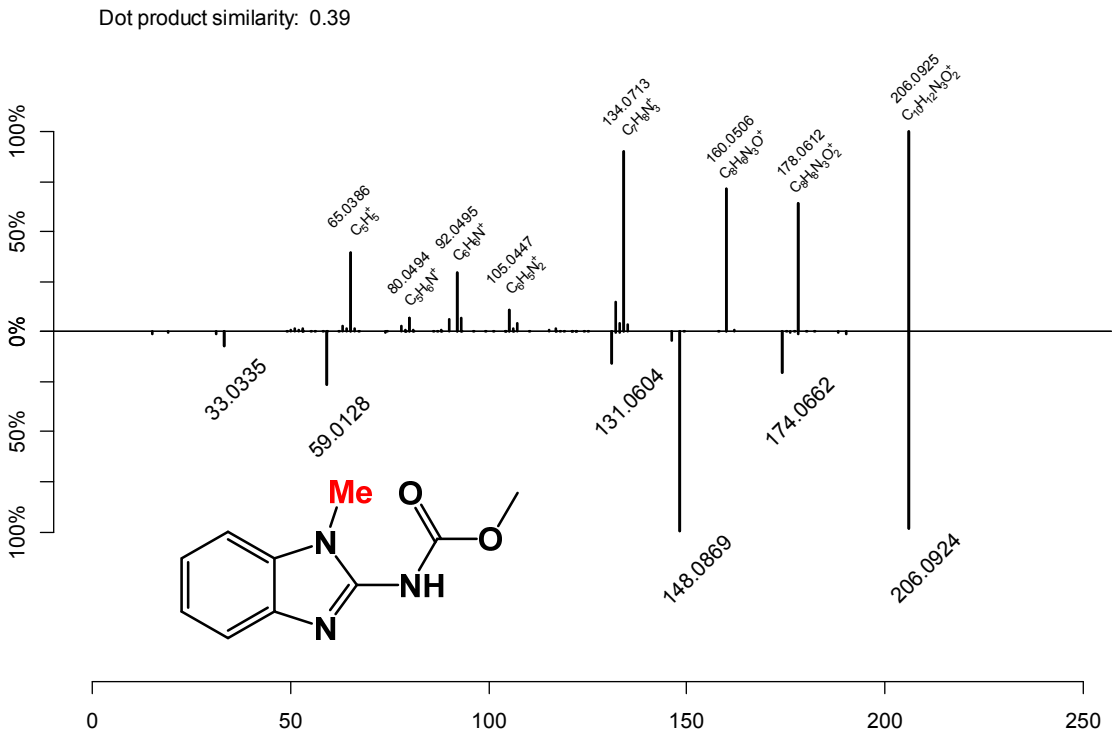

Top: MS2 spectrum, positive mode, parent $[M+H]^+$ 206.0924, merged spectra (collision energies NCE 15, 30, 45, 60, 75, 90) by absolute intensity. MassBank reference: ET270101-ET270109.

Bottom: In-silico MS2 spectrum, CFM-ID, positive mode, merged spectra (collision energy 10 eV, 20 eV, 40 eV).

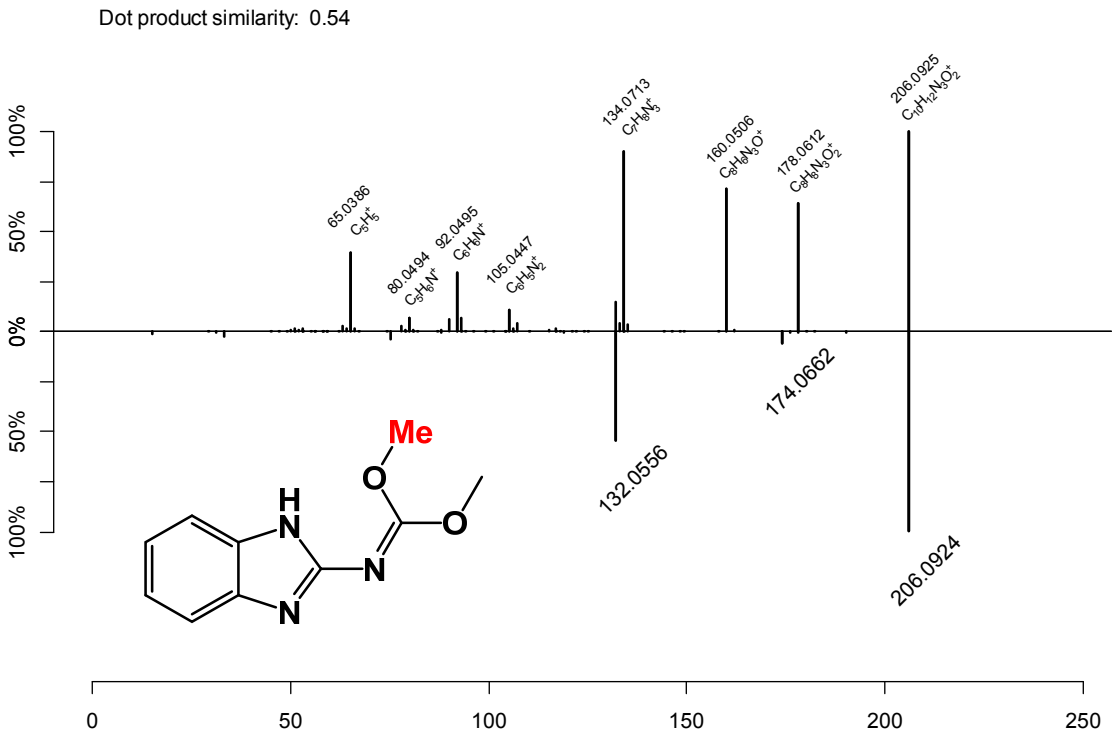

Top : MS2 spectrum, positive mode, parent $[M+H]^+$ 206.0924, merged spectra (collision energies NCE 15, 30, 45, 60, 75, 90) by absolute intensity. MassBank reference: ET270101-ET270109.

Bottom: In-silico MS2 spectrum, CFM-ID, positive mode, merged spectra (collision energy 10 eV, 20 eV, 40 eV).

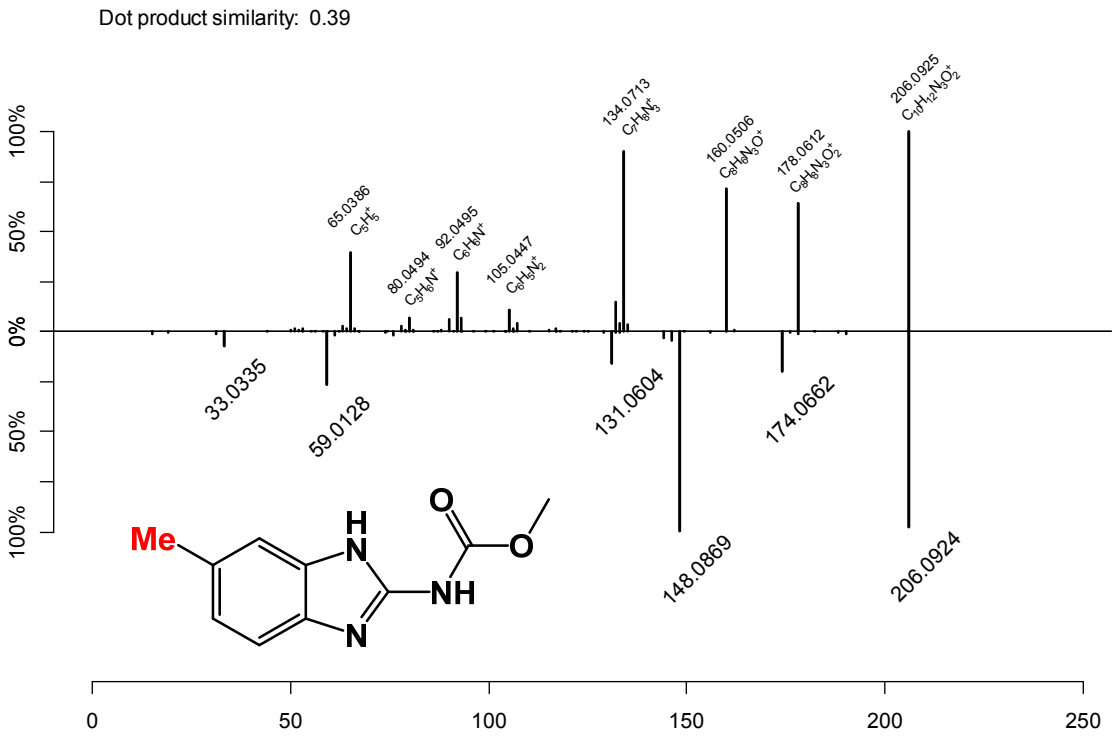

S3.4 Structure elucidation of SMZ-Pt

MS2 spectrum, positive mode, parent $[M+H]^+$ 429.1090, merged spectra (collision energy NCE 15, 30, 45, 60, 75, 90, 120, 150, 180). Automated formula annotation (RMassBank) MassBank reference: ET310201-ET310209.

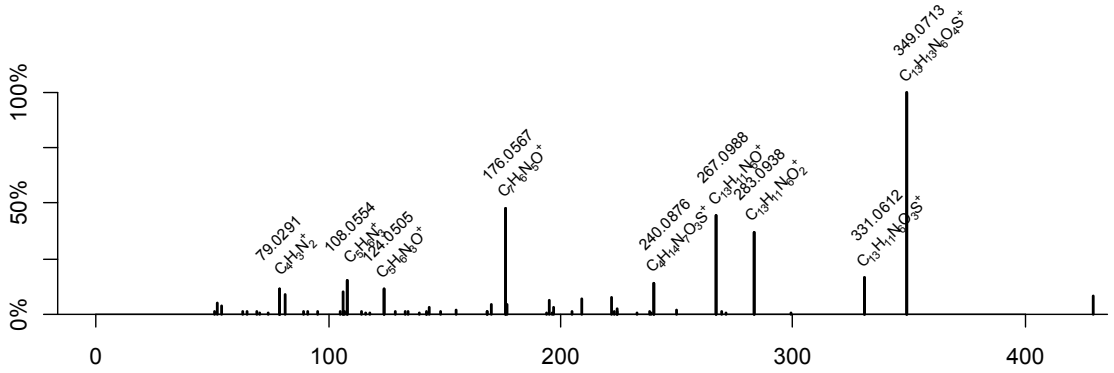

Proposed Structure (modification in red) **and Fragmentation:**

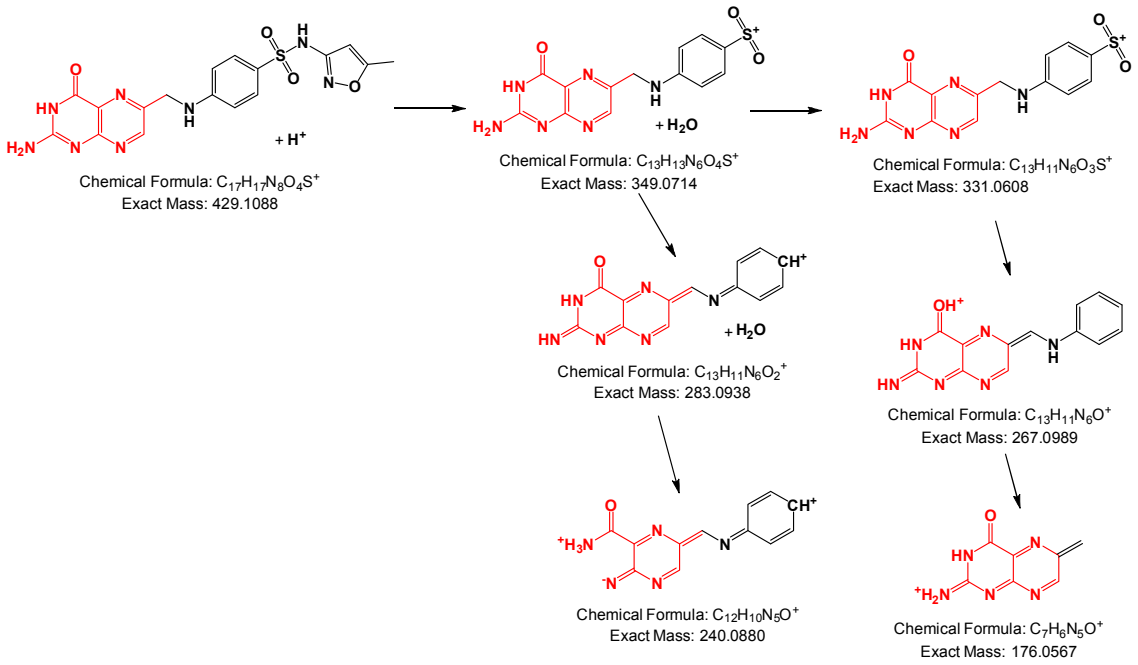

Confidence level: Level 2b

Additional evidence for structure interpretation:

Fragment 331.0612 corresponds to documented fragment 331.0606 as found by Richter et al.[18]

Note: Gas-phase addition of residual H_2O to fragments has been documented e.g. for guanine and guanosine [19,20]

S3.5 Structure elucidation of SMZ-PtO

MS2 spectrum, positive mode, parent $[M+H]^+$ 430.0930, merged spectra (collision energy NCE 15, 30, 45, 60, 75, 90, 120, 150, 180). Automated formula annotation (RMassBank). MassBank reference: ET310301-ET310309.

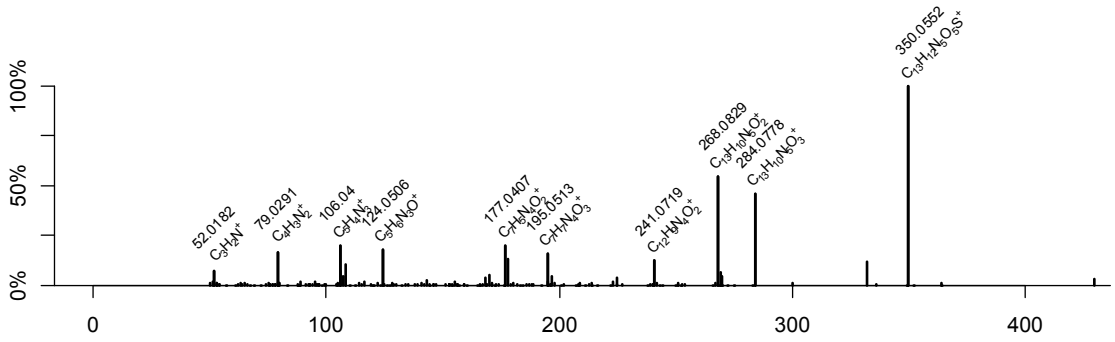

Proposed Structure (modification in red) **and Fragmentation:**

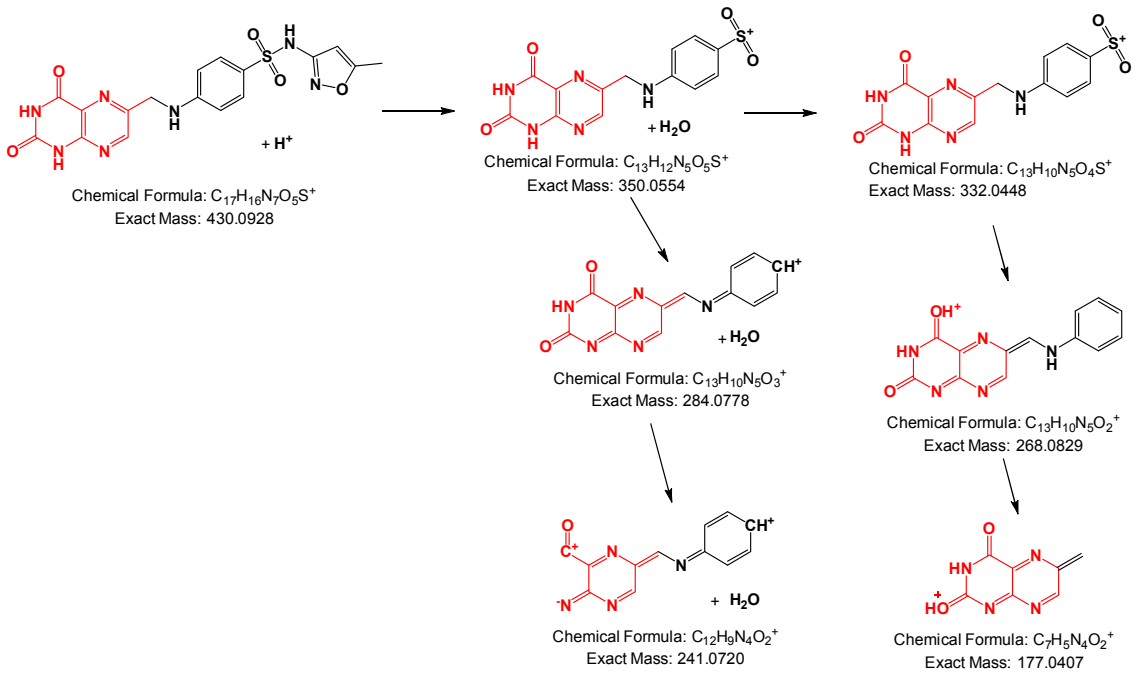

Confidence level: Level 3

Additional evidence for structure interpretation:

Compare to SMZ-Pt.

Note: Gas-phase addition of residual H_2O to fragments has been documented e.g. for guanine and guanosine[19,20]

S3.6 Structure elucidation of SMZ-AcOH

MS2 spectrum, positive mode, parent $[M+H]^+$ 312.0649, collision energy NCE 30. Automated formula annotation (RMassBank). MassBank reference: ET310402.

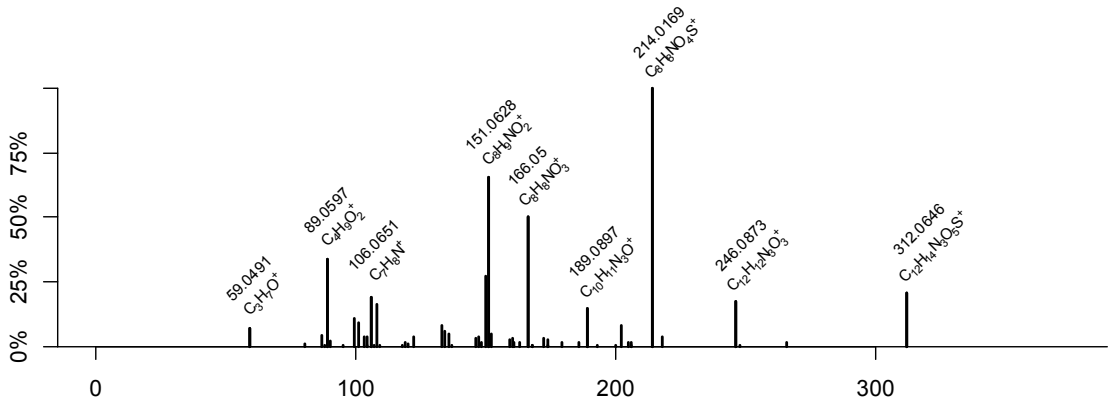

Proposed Structure (modification in red) **and Fragmentation:**

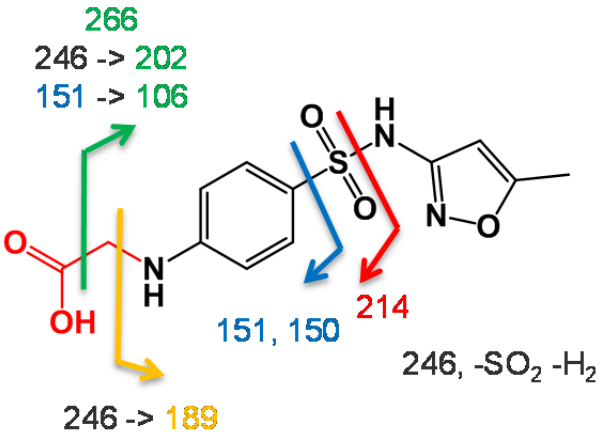

Confidence level: Level 3

Additional evidence for structure interpretation:

Does not coelute with an authentic standard of N4-hydroxyacetyl-sulfamethoxazole.

Peak 166.0500 corresponds to the peak 108.0444 in SMZ, which arises through rearrangement. SO_2 loss rearrangements in analogy to SMZ. Peaks 151, 150 correspond to peaks 93, 92 in SMZ.

S3.7 Structure elucidation of BEZ-da

MS2 spectrum, positive mode, parent $[M+H]^+$ 276.0786, collision energy NCE 45. Automated formula annotation (RMassBank). MassBank reference: ET290103.

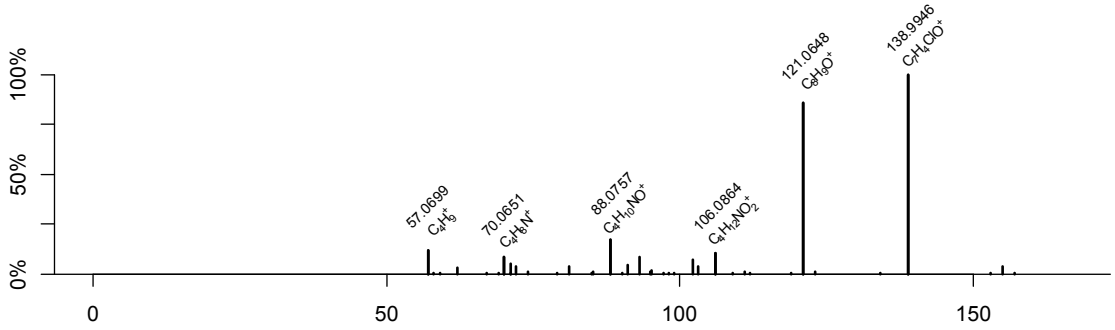

Proposed Structure (modification in red) **and Fragmentation:**

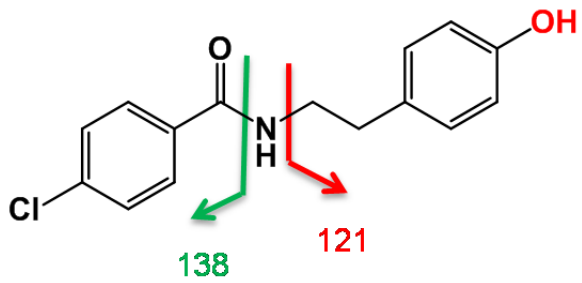

Confidence level: Level 2b

Additional evidence for structure interpretation:

Compare to BEZ (MassBank EA020909), fragments 138, 121.

Note: Spectrum is deconvoluted by RMassBank from co-fragmenting m/z 276.2803. m/z 57, 70, 88, 106 are likely ambiguous fragments incorrectly attributed to BEZ-da.

S3.8 Structure elucidation of BEZ-M

MS2 spectrum, positive mode, parent $[M+H]^+$ 376.1310, collision energy NCE 30. Automated formula annotation (RMassBank). MassBank reference: ET290202.

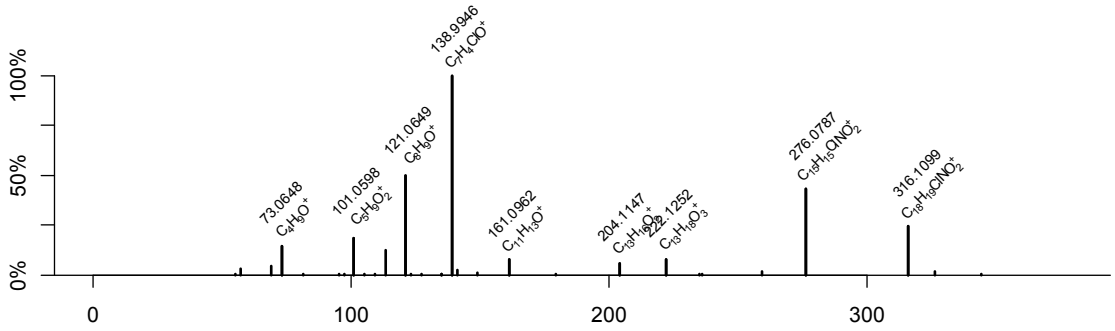

Proposed Structure (modification in red) **and Fragmentation:**

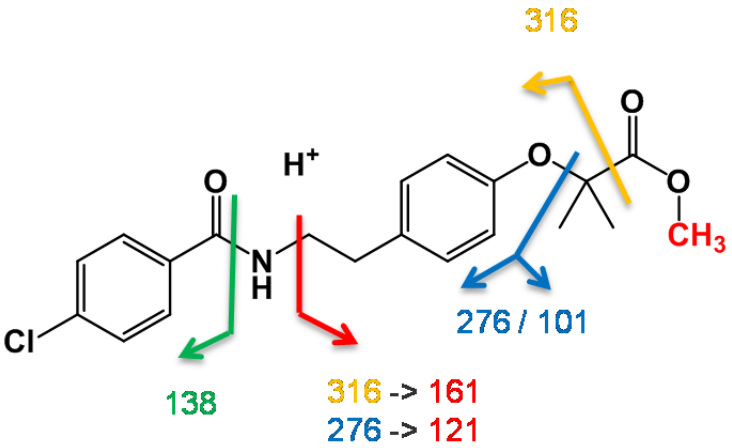

Confidence level: Level 2b

Additional evidence for structure interpretation:

Compare to BEZ (MassBank EA020909), fragments 316, 276, 161, 138, 121 structurally shared, fragment 101 structurally specific to TP.

S3.9 Structure elucidation of RAN-dm

Top : MS2 spectrum, positive mode, parent $[M+H]^+$ 301.1329, collision energy NCE 30. Automated formula annotation (RMassBank). MassBank reference: ET300102.

Bottom: Library MS2 spectrum, ranitidine, $[M+H]^+$ 315.1485, collision energy NCE 30. Automated formula annotation (RMassBank). MassBank reference: EA019603.

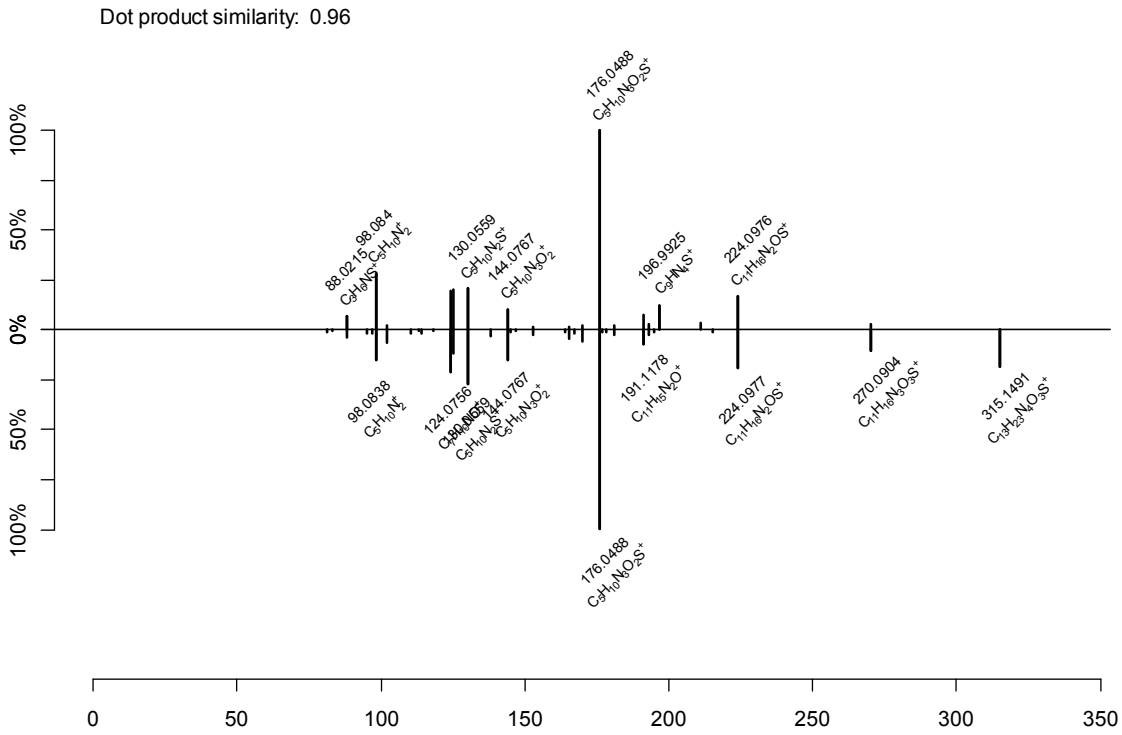

Proposed Structure (modification in red) **and Fragmentation:**

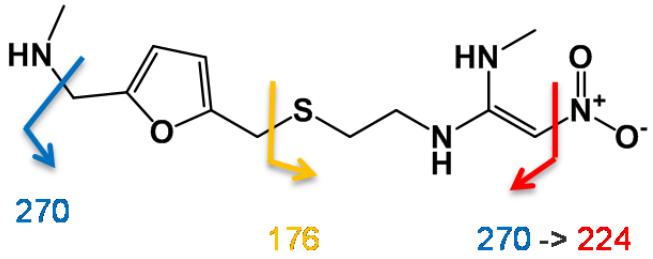

Confidence level: Level 2b

Additional evidence for structure interpretation:

The loss of NHCH3 (m/z 270) is diagnostic for the mono-demethylation on the dimethyl-N. Fragment 176 is diagnostic for the retention of methyl on the monomethyl-N.

S3.10 Structure elucidation of MPL-dm

Top : MS2 spectrum, positive mode, parent $[M+H]^+$ 254.1750, collision energy NCE 30. Automated formula annotation (RMassBank). MassBank reference: ET280102.

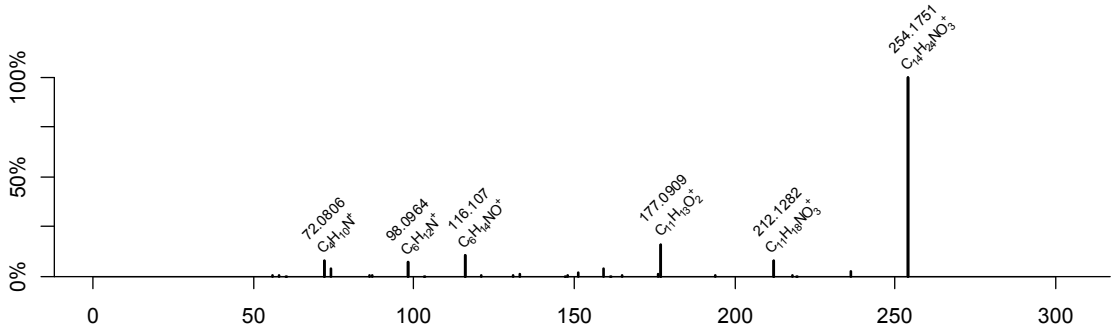

Proposed Structure (modification in red) **and Fragmentation:**

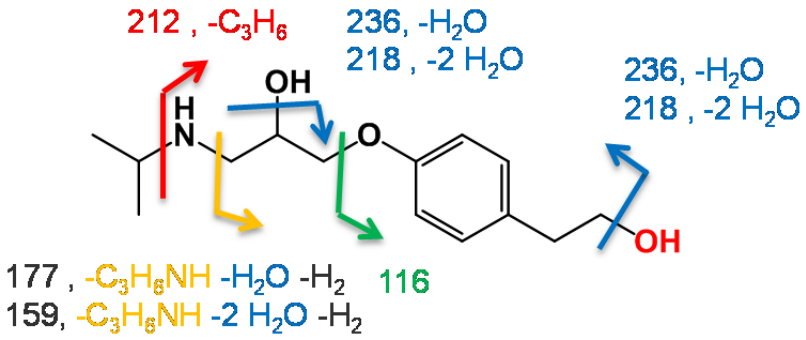

Confidence level: Level 2b

Additional evidence for structure interpretation:

Compare to MPL (MassBank EA017201..14)

References

1 R. R. L. Guillard and C. J. Lorenzen, *J. Phycol.*, 1972, **8**, 10–14.
2 V. M. Markowitz, I.-M. A. Chen, K. Palaniappan, K. Chu, E. Szeto, M. Pillay, A. Ratner, J. Huang, T. Woyke, M. Huntemann, I. Anderson, K. Billis, N. Varghese, K. Mavromatis, A. Pati, N. N. Ivanova and N. C. Kyrpides, *Nucleic Acids Res.*, 2014, **42**, D560–D567.
3 V. M. Markowitz, I.-M. A. Chen, K. Chu, E. Szeto, K. Palaniappan, M. Pillay, A. Ratner, J. Huang, I. Pagani, S. Tringe, M. Huntemann, K. Billis, N. Varghese, K. Tennessen, K. Mavromatis, A. Pati, N. N. Ivanova and N. C. Kyrpides, *Nucleic Acids Res.*, 2014, **42**, D568–D573.
4 K. A. Lewis, J. Tzilivakis, D. J. Warner and A. Green, *Hum. Ecol. Risk Assess. Int. J.*, 2016, **22**, 1050–1064.
5 D. S. Wishart, *Nucleic Acids Res.*, 2006, **34**, D668–D672.
6 National Center for Biotechnology Information, .
7 US EPA, *Estimation Programs Interface Suite™ for Microsoft® Windows, v 4.11*, United States Environmental Protection Agency, Washington, DC, USA., 2016.
8 K. Harada, S. Imanishi, H. Kato, M. Mizuno, E. Ito and K. Tsuji, *Toxicon*, 2004, **44**, 107–109.
9 F. Allen, R. Greiner and D. Wishart, *Metabolomics*, 2014, **11**, 98–110.
10 F. Allen, A. Pon, M. Wilson, R. Greiner and D. Wishart, *Nucleic Acids Res.*, 2014, **42**, 94–99.
11 M. R. Bauerle, E. L. Schwalm and S. J. Booker, *J. Biol. Chem.*, 2015, **290**, 3995–4002.
12 C. S. Boyer and D. R. Petersen, *J. Pharmacol. Exp. Ther.*, 1992, **260**, 939–946.
13 S. Kern, R. Baumgartner, D. E. Helbling, J. Hollender, H. Singer, M. J. Loos, R. P. Schwarzenbach and K. Fenner, *J. Environ. Monit.*, 2010, **12**, 2100–11.
14 M. Skiba, M. Skiba-Lahiani, H. Marchais, R. Duclos and P. Arnaud, *Int. J. Pharm.*, 2000, **198**, 1–6.
15 E. Rott, *Schweiz. Z. Für Hydrol.*, 1981, **43**, 34–62.
16 C. S. Reynolds, *Ecology of phytoplankton*, Cambridge University Press, Cambridge; New York, 2006.
17 AstraZeneca, *Environmental Risk Assessment Data: Atenolol*, 2013.
18 M. K. Richter, A. Focks, B. Siegfried, D. Rentsch, M. Krauss, R. P. Schwarzenbach and J. Hollender, *Environ. Pollut.*, 2013, **172**, 208–15.
19 R. Tuytten, F. Lemière, W. Dongen, E. L. Esmans, E. Witters, W. Herrebout, B. Veken, E. Dudley and R. P. Newton, *J. Am. Soc. Mass Spectrom.*, 2005, **16**, 1291–1304.
20 J. Sultan, *Int. J. Mass Spectrom.*, 2008, **273**, 58–68.